

Femtosecond laser processing of fiber Bragg gratings with photo-induced gradient-index assisted focusing

This content has been downloaded from IOPscience. Please scroll down to see the full text.

2014 J. Micromech. Microeng. 24 075015

(<http://iopscience.iop.org/0960-1317/24/7/075015>)

View [the table of contents for this issue](#), or go to the [journal homepage](#) for more

Download details:

IP Address: 117.32.153.137

This content was downloaded on 18/06/2014 at 02:46

Please note that [terms and conditions apply](#).

Femtosecond laser processing of fiber Bragg gratings with photo-induced gradient-index assisted focusing

Wei Cui, Tao Chen, Jinhai Si, Feng Chen and Xun Hou

Key Laboratory for Physical Electronics and Devices of the Ministry of Education & Shaanxi Key Lab of Information Photonic Technique, Collaborative Innovation Center of Suzhou Nano Science and Technology, School of Electronics & Information Engineering, Xi'an Jiaotong University, No. 28, Xianning West Road, Xi'an, 710049, People's Republic of China

E-mail: jinhaisi@mail.xjtu.edu.cn

Received 10 February 2014, revised 17 April 2014

Accepted for publication 9 May 2014

Published 9 June 2014

Abstract

Gradient-index modulation prefabrication in the cladding of standard telecom fibers was proposed for femtosecond laser processing of Type II-IR fiber Bragg gratings. The refractive index of the prefabricated region in the cladding had a large gradient across the laser beam, which could act as a cylindrical lens to enhance the focusing of laser beam when writing Type II-IR gratings. With the help of prefabrication, the threshold pulse energy for processing Type II-IR FBGs was lowered from $750\mu\text{J}$ to $520\mu\text{J}$. The fabricated FBGs showed good thermal stability at temperatures over 900°C .

Keywords: fiber Bragg gratings, femtosecond laser processing, gradient index

(Some figures may appear in colour only in the online journal)

1. Introduction

Fiber Bragg gratings (FBGs) have been broadly used in the telecommunication, laser and sensing fields [1, 2]. They are high precision, compact and easy to multiplex, making them strong competitors to conventional electronic sensors for applications such as temperature and strain measurements. Femtosecond infrared (IR) laser systems have been proved to be useful for processing FBGs in recent years [3]. They can be used to fabricate FBGs in various optical fibers without special photosensitization [4, 5], due to their high peak intensities and the strong nonlinear interaction between light and materials [6]. When combined with the phase mask technique, they give a highly repeatable spatially modulated interference field and ease of alignment. There are two types of induced refractive index modulation in FBG processing using femtosecond IR lasers [7]. Type I-IR FBGs result from defect formation due to multiphoton absorption, whose maximum operating temperature does not exceed 500°C . Type II-IR FBGs are due to localized melting or void formation resulting from the multiphoton ionization (MPI). Type II-IR FBGs exhibit permanent performance up to the glass

transition temperature, making them suitable for sensing applications in harsh environments.

The writing of Type II-IR FBGs using a femtosecond IR laser and a phase mask was first reported in 2004 by Smelser [8], in which high laser pulse energies over 1 mJ were needed, and the fiber had to be placed very close to the phase mask to take advantage of the multiple beam interference and increase the laser intensity at the fiber core [9, 10]. However, when the phase mask is close to the fiber, the nonlinear absorption in the phase mask, which is due to the high laser intensity, would shorten the lifetime of the costly phase mask or damage it. Furthermore, the self-focusing effect in the phase mask would disturb the alignment of the focal spot and the fiber core [11]. When a 25 mm cylindrical lens is used and the distance between the focal point and the phase mask is set at $400\mu\text{m}$, a pulse energy over $950\mu\text{J}$ would result in significant self-focusing; even white light generation is in the phase mask.

In this paper, gradient-index (GRIN) modulation prefabrication in the cladding of standard telecom fibers was proposed for femtosecond laser processing of Type II-IR FBGs. The refractive index of the prefabricated region in the cladding had a large gradient across the laser beam, which

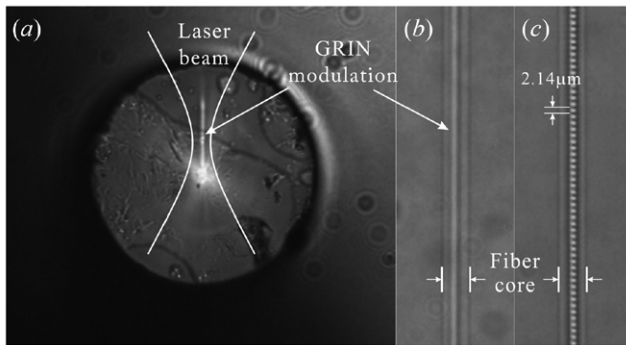


Figure 1. (a) Cross-sectional morphology of the prefabricated GRIN modulation area. (b) Axial morphology of GRIN modulation area viewed along the beam axis. (c) Grating fringes fabricated with GRIN-assisted focusing.

could act as a cylindrical lens to enhance the focusing of the laser beam when writing Type II-IR gratings. With GRIN-assisted focusing, the laser power threshold for writing Type II-IR FBGs was lowered from $750\mu\text{J}$ to $520\mu\text{J}$. The annealing behavior of the fabricated FBG was studied. The FBG showed good thermal stability at temperatures over 900°C .

2. Experiment setups

Femtosecond laser pulses with 150-fs duration were generated by an amplified Ti:sapphire laser at a center wavelength of 800 nm and 1 kHz repetition rate. It has maximum output energy of about 1 mJ. The 12 mm diameter Gaussian beam was focused with a 25 mm cylindrical lens through a zero-order nulled phase mask with a period $\Lambda_m = 2.14\mu\text{m}$ into the standard telecom fiber core. According to free space Gaussian beam optics, the width of the focal spot size is $W = 2\omega \approx 2\lambda f / \pi\omega_0 = 2.1\mu\text{m}$, where λ is the wavelength, f is the focal length of the cylindrical lens, and ω_0 is the incident beam waist. The focus area was $2.1\mu\text{m} \times 10\text{mm}$. The distance between fiber and phase mask was set to $400\mu\text{m}$ to produce a multiple beam interference-field pattern with higher intensity than that generated by two-beam interference [12].

In our method, the femtosecond laser beam was focused on the cladding through the cylindrical lens without a phase mask before writing gratings. When the pulse energy was set at $700\mu\text{J}$, the fiber was exposed for 60 seconds to prefabricate the GRIN modulation area, in which the laser-induced index modulation would reach its saturation value. The laser intensity was estimated to be $3 \times 10^{13}\text{W}/\text{cm}^2$, which could induce Type I-IR index change [8]. Due to the energy distribution of Gaussian laser beam, the index would have a large gradient along the horizontal direction in the prefabricated area. Figure 1(a) shows the cross-sectional morphology of the GRIN modulation area in the fiber. The GRIN modulation area was located in the cladding and extended into the core. The area is about $45\mu\text{m}$ in length and $3\mu\text{m}$ in width. Figure 1(b) shows the axial morphology of the GRIN modulation area viewed along the laser beam axis. The prefabricated index modulation would result in some influence on FBGs, such as increasing the dc index modulation of FBGs and cladding-mode coupling loss,

the value of which was about 1×10^{-3} and -3dB , respectively. But the GRIN modulation can be eliminated by an annealing process after writing gratings, because the GRIN modulation resulted from a Type I-IR index change. The GRIN modulation area could act as a second cylindrical lens for focusing the writing beam to increase the intensity. After the prefabrication of the GRIN modulation, the laser was blocked. The phase mask was mounted and the distance between fiber and phase mask was set to $400\mu\text{m}$. The cylindrical lens would be realigned to make the interference pattern focused into the core through the GRIN modulation area. A translation stage with differential adjusters and piezo actuators was used, the resolution of which was $0.5\mu\text{m}$ and 20nm , respectively. The symmetry of the transmission light pattern could be used to confirm the alignment, which was very sensitive to the fiber position. The error in the alignment was estimated to be about $0.2\mu\text{m}$. Then the fiber would be exposed for 20 seconds to write the gratings. Figure 1(c) shows the axial morphology of the fabricated Type II-IR FBG viewed along the laser beam axis. The grating pitch is $\Lambda_G = \Lambda_m = 2.14\mu\text{m}$, which is caused by the multiple beam interference.

3. Experiment and result

3.1. Threshold study

The threshold pulse energy for processing Type II-IR FBGs using the common and GRIN-assisted focusing method was measured, respectively. The exposure conditions and setups were the same as described earlier, despite the lack of GRIN modulation prefabrication in the common method. To determine the threshold, the pulse energy was increased until white light generation occurred in the fiber coincident with Type II-IR grating formation. The white light generation threshold pulse energy using the common method was determined to be $750\mu\text{J}$, while the white light generation threshold pulse energy using the GRIN-assisted focusing was $520\mu\text{J}$. The result indicates that threshold pulse energy for fabrication of Type II-IR gratings is reduced to about 69%.

Type II-IR FBGs were fabricated using the common method and GRIN modulation-assisted focusing method, respectively, in which pulse energy was set at $800\mu\text{J}$. Figure 2 shows the reflection spectra of the FBGs fabricated using the common method and the GRIN modulation-assisted focusing method. From figure 2, we can see that the Bragg wavelength of the FBG fabricated using the common method and GRIN modulation-assisted focusing method was 1549.9nm and 1550.9nm , respectively, which was because the prefabrication increased the dc index modulation. It should be noticed that the peak reflectivity for the two FBGs was close to -3dB , which can be explained as follows. In the FBG fabricated without prefabrication, a hybrid FBG including Type I-IR gratings was fabricated, in which about 1.5 mm long Type II-IR gratings in the center region and Type I-IR gratings in the two side regions were observed. The total length of the FBG was measured to be about 3.8 mm. When the GRIN modulation-assisted focusing method was used, the length of the fabricated Type II-IR FBG was increased to about 3.5 mm. There were no Type

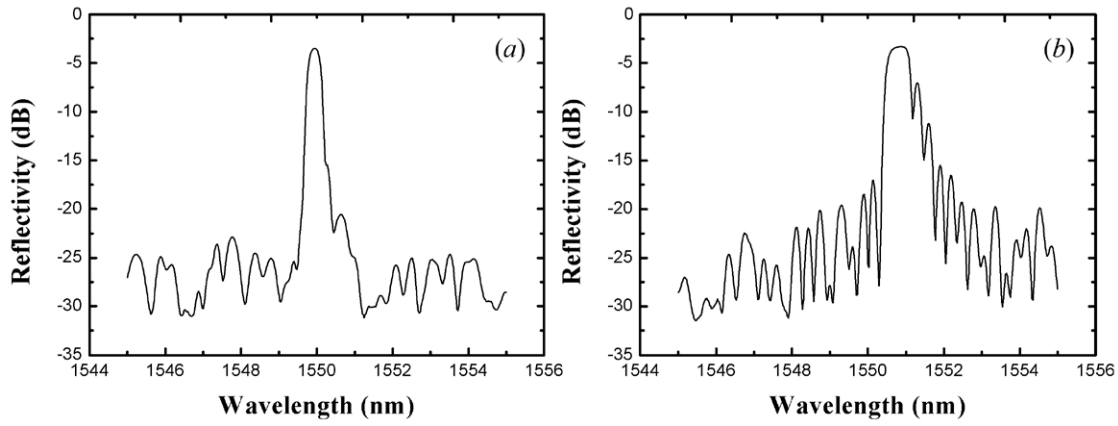


Figure 2. Reflection spectra of the FBGs fabricated using the common method (a) and the GRIN modulation-assisted focusing method (b).

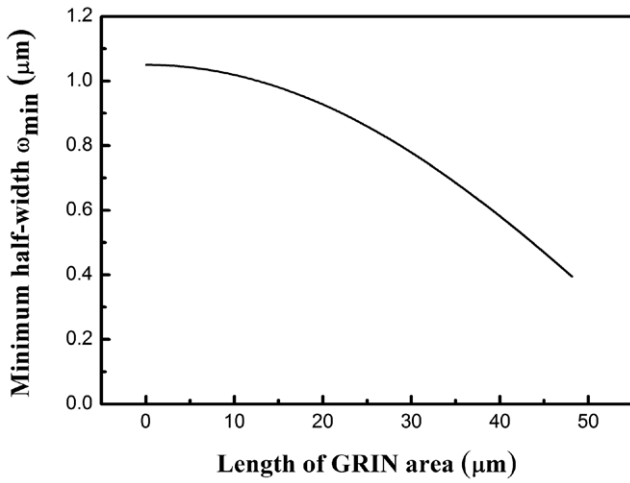


Figure 3. Variation of minimum beam half-width ω_{min} with the length of GRIN area.

I-IR gratings in the side region, because the Type I-IR index change was almost saturated during the prefabrication.

We investigated the focusing of a writing beam propagating through the GRIN area by numerical calculation. We assumed that the incident beam is oriented along the y-axis and the gradient direction is oriented along the x-axis. The spatial refractive index profile of the prefabricated area should be complex, due to the multiphoton absorption process and self-focusing effect. It could be determined using differential interference contrast imaging for accurate analysis [13]. To simplify the calculation, we assume that the refractive index distribution within the GRIN area is given by the following equations [14]:

$$n(x) = (n_0 + \Delta n) \left(1 - \frac{g_0^2 x^2}{2} \right)$$

$$g_0^2 = \frac{8\Delta n}{d^2(n_0 + \Delta n)}$$

where Δn denotes the index modulation in the center of the modified area. In our case the maximum Type I-IR index modulation is about 1×10^{-3} and g_0 denotes the gradient parameter. The width of the GRIN modulation area d is about $3 \mu\text{m}$ according to the microscope image. The refractive index of

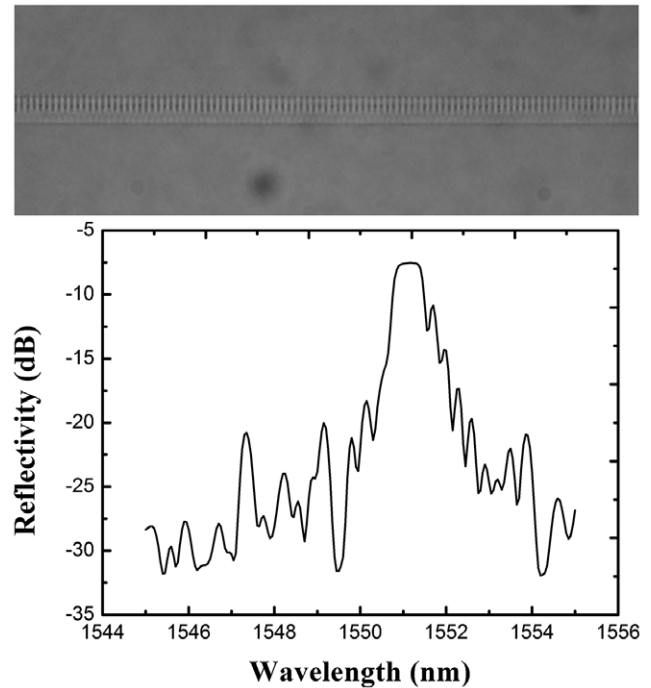


Figure 4. Image and reflection spectrum of Type II gratings fabricated using GRIN-assisted focusing. The separation distance between the phase mask and the fiber was 1.2 mm.

the cladding is $n_0=1.4628$. The behavior of a Gaussian beam in the gradient index media also depends on beam waist radius ω_i and waist position s_i of the incident Gaussian. The waist radius of the incident Gaussian beam after being focused by cylindrical lens was $\omega_i=1.05 \mu\text{m}$. The half-width of a Gaussian beam that propagates along the y-axis is given by

$$\omega^2(s_i, y) = \omega_i^2 \left\{ \cos^2(g_0 y) + \left[\frac{\lambda}{(n_0 + \Delta n) \pi \omega_i^2} \right]^2 \left[\frac{\sin(g_0 y)}{g_0} + s_i \cos(g_0 y) \right]^2 \right\}$$

By numerical calculation we can obtain the curve of minimum beam half-width ω_{min} versus the length of GRIN modulation area, which is shown in figure 3. Considering the length of the fabricated GRIN area is about $45 \mu\text{m}$, and the $8 \mu\text{m}$ diameter fiber core is at the end of the area, we assume

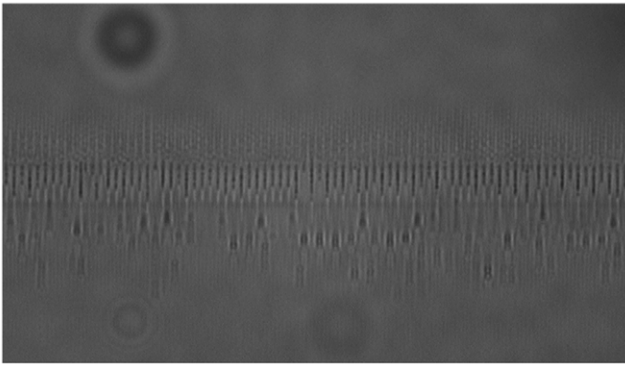


Figure 5. Image of the Type II-IR FBG fabricated using GRIN-assisted focusing for annealing study.

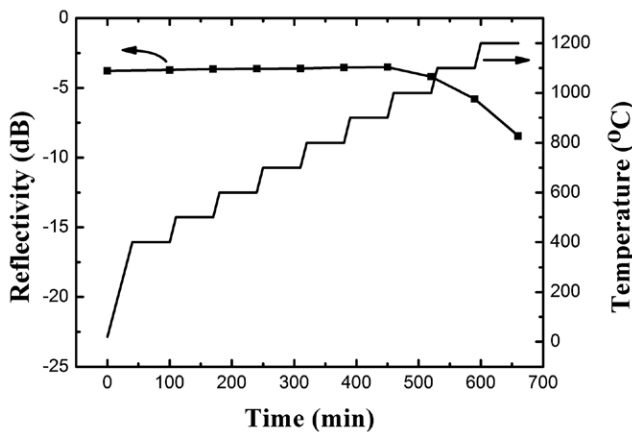


Figure 6. Variation of the reflectivity (square) of the FBG and the temperature (solid line) of the tube furnace in the short-term annealing treatment.

that the effective length of GRIN area is $37\mu\text{m}$. The ω_{min} could be reduced to $0.652\mu\text{m}$ (62% of the original value), as shown in figure 3, which is in good agreement with the experiment result.

With the help of the GRIN-assisted focusing, Type II-IR FBGs could be achieved using a larger separation distance between the phase mask and the fiber. The pulse energy was set to $900\mu\text{J}$. The maximum separation distance for processing Type II-IR FBGs using common and GRIN-assisted focusing method was measured, respectively. The distance between the phase mask and the fiber was decreased from 2 mm until white light occurred. The maximum separation distance using common method and GRIN-assisted focusing method was determined to be about $500\mu\text{m}$ and 1.2 mm, respectively. Figure 4 shows the image and reflection spectrum of the fabricated FBG using GRIN-assisted focusing, in which the separation distance between the phase mask and the fiber is 1.2 mm. The nonlinear absorption in the phase mask can be reduced at the 1.2 mm separation distance.

3.2. Annealing study

To investigate the thermal stability of the Type II-IR FBGs fabricated using this method, we used a short-term annealing

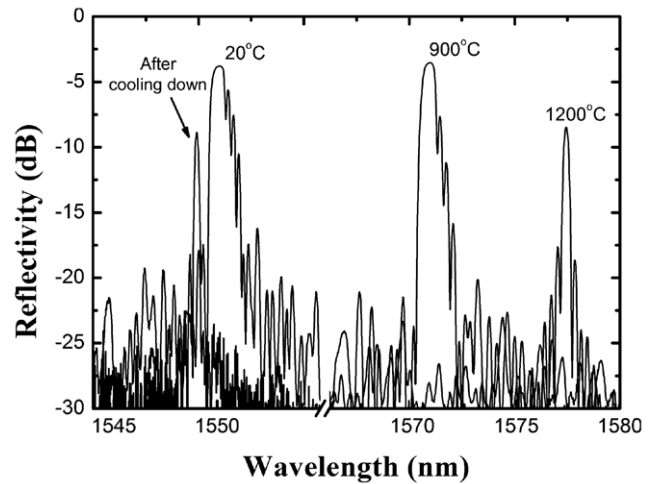


Figure 7. Reflection spectra of the FBG at 20°C, 900°C, 1200°C and after cooling down, respectively.

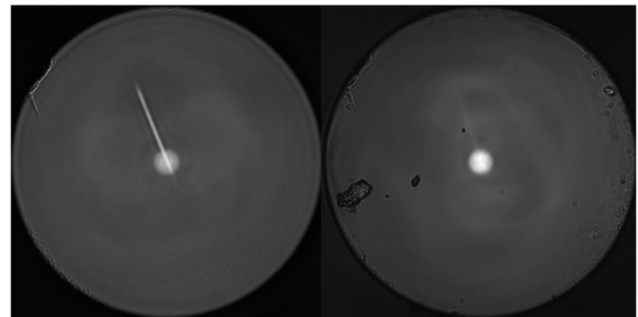


Figure 8. Cross-sectional morphology of the prefabricated GRIN modulation area before (left) and after (right) the annealing process.

treatment with a tube furnace. The FBG was processed using the same method as described above. The pulse energy was increased to $800\mu\text{J}$ from $520\mu\text{J}$ to increase the grating length, which would offer better SNR for the spectrum analysis during the annealing study. Figure 5 shows the image of the FBG fabricated for the annealing study. The FBG was subjected to short-term thermal exposure (60 min at each temperature) at 400°C, 500°C, and then progressively to 1200°C with a temperature increment of 100°C. The variation of reflectivity and temperature are shown in figure 6. The reflectivity increased slightly from -3.78 dB to -3.51 dB with temperature increasing from room temperature to 900°C. At 1200°C the reflectivity decreased to -8.45 dB (34% of the initial reflectivity). The reflection spectra of the FBG at 20°C, 900°C, 1200°C and after cooling down are shown in figure 7, respectively.

To prove that the prefabricated GRIN modulation could be eliminated by annealing process, fiber with GRIN prefabrication was subjected to short-term exposure at 850°C and stabilized for five hours. Figure 8 shows the cross-sectional morphology of the prefabricated GRIN modulation area before and after the annealing process. The result suggests that the annealing process is able to eliminate the prefabricated GRIN modulation.

4. Conclusion

In conclusion, we have presented a method using prefabricated GRIN modulation for femtosecond laser processing of Type II-IR FBGs in standard telecom fibers. With the GRIN-assisted focusing, the laser threshold pulse energy for writing Type II-IR FBGs was lowered from $750\mu\text{J}$ to $520\mu\text{J}$. The annealing behavior of the fabricated FBGs was studied. The FBGs showed good thermal stability at temperatures over 900°C . The result also suggests the Type I-IR GRIN modulation could be eliminated by an annealing process.

Acknowledgements

The authors gratefully acknowledge the financial support for this work provided by the National Basic Research Program of China (973 Program) under Grant No. 2012CB921804, and the National Natural Science Foundation of China (NSFC) under the Grant Nos. 11204236 and 61235003, and Opened Fund of the State Key Laboratory on Integrated Optoelectronics No. IOSKL2012KF.

References

- [1] Rao Y 1999 In-fibre bragg grating sensors *Meas. Sci. Technol.* **8** 355
- [2] Giles C R 1997 Lightwave applications of fiber bragg gratings *J. Light. Technol.* **15** 1391–04
- [3] Martinez A et al 2004 Direct writing of fibre bragg gratings by femtosecond laser *Electron. Lett.* **40** 1170–2
- [4] Mihailov S J et al 2003 Fiber bragg gratings made with a phase mask and 800 nm femtosecond radiation *Opt. Lett.* **28** 995–7
- [5] Mihailov S J et al 2011 Bragg grating inscription in various optical fibers with femtosecond infrared lasers and a phase mask *Opt. Mater. Express* **1** 754–65
- [6] Davis K M et al 1996 Writing waveguides in glass with a femtosecond laser *Opt. Lett.* **21** 1729–31
- [7] Sudrie L et al 2001 Study of damage in fused silica induced by ultra-short IR laser pulses *Opt. Commun.* **191** 333–9
- [8] Smelser C, Mihailov S and Grobncic D 2005 Formation of Type I-Ir and Type II-Ir gratings with an ultrafast Ir laser and a phase mask *Opt. Express* **13** 5377–86
- [9] Smelser C W et al 2004 Multiple-beam interference patterns in optical fiber generated with ultrafast pulses and a phase mask *Opt. Lett.* **29** 1458–60
- [10] Changrui L et al 2010 Morphology and thermal stability of fiber bragg gratings for sensor applications written in h_2 -free and h_2 -loaded fibers by femtosecond laser *J. IEEE Sensors* **10** 1675–81
- [11] Shen Y 1984 *The principles of nonlinear optics* (New York: Wiley-Interscience) pp 303–31
- [12] Smelser C W, Grobncic D and Mihailov S J 2004 Generation of pure two-beam interference grating structures in an optical fiber with a femtosecond infrared source and a phase mask *Opt. Lett.* **29** 1730–32
- [13] Kouskousis B P et al 2006 Quantitative investigation of the refractive-index modulation within the core of a fiber Bragg grating *Opt. Express* **14** 10332–8
- [14] Gómez-Reino C, Perez M V and Bao C 2002 *Gradient-index optics: fundamentals and applications* (Springer)